A gain scheduled H-infinity controller for a re-entry benchmark

Andrés Marcos*
Deimos Space S.L., Madrid, 28760, Spain

In this paper we present the design process and results for a re-entry baseline controller used as a benchmarking reference within a European Space Agency (ESA) project on advanced gain-scheduling techniques. The controller is based on output gain-scheduling of a set of LTI H_∞ controllers obtained using a decoupled motion approach. The rationale behind the selection of the design points, and the analyses and guidelines used in the design and tuning of the controllers to satisfy the desired global performance and robustness objectives are described in detail. The re-entry vehicle used is an enhanced version of the well-known NASA HL-20 based on a detailed NASA aerodynamic database and including nonlinear actuators, colored sensor models, realistic uncertainties and a control mix logic. The latter logic fully couples the longitudinal and lateral/directional motions while the noise and uncertainties used are key in making of this enhanced HL20 a realistic benchmark for re-entry control design.

I. Introduction

Gain scheduling is a standard industrial methodology to design controllers for dynamical systems over a wide performance envelope [416, 17, 18]. In its most commonly used approach, it yields a global controller based on interpolation of a family of locally linearized controllers –each designed around a linear time invariant (LTI) representation of the plant. If the linear models change dramatically at each operating point due to uncertainty variations this implies an increase on the complexity of the local controller (due to the need to satisfy more demanding robustness objectives at each point) and of the global gain-scheduled controller (due to the overall scheduling scheme). Furthermore, mission profiles and vehicles with large parametric or non-parametric uncertainty can be tackled with classical gain scheduling techniques but only after numerous ad hoc analyses that try to ensure the stability and performance for such wide variations. The combination of traditional gain-scheduling with robust modern control design methods such as H_∞ can help alleviate some of the (local) robustness issues without increasing the complexity in the gain-scheduling of the global controller. Compared with more advanced gain-scheduling approaches, such as linear parameter varying (LPV) methods, the advantage of H_∞ gain-scheduling is that it is more readily connected with traditional industrial practices.

In this article the design process and results for a re-entry baseline controller used as a benchmarking reference within a European Space Agency (ESA) project on advanced gain-scheduling techniques is presented. The controller is based on output gain-scheduling of a set of LTI $H\infty$ controllers obtained using a decoupled motion approach. The rationale behind the selection of the design points, and the analyses and guidelines used in the design and tuning of the controllers to satisfy the desired global performance and robustness objectives are described in detail.

The article is divided as follows. Section II presents the LPVMAD project as well as the re-entry benchmark developed. Section III details the longitudinal and lateral/directional baseline controller design. Section IV presents the linear and pseudo-linear (i.e. with nonlinear components) analyses performed during the design cycle in order to validate the desired robustness and performance properties. Section V presents the nonlinear time simulations of the full motion baseline controller in the nonlinear re-entry benchmark simulator, including noise and challenging uncertainty profiles. Section VI concludes with a summary of the results.

* Deimos Space S.L.U. Email: andres.marcos@deimos-space.com. AIAA senior member.

II. LPVMAD project and re-entry benchmark

The European Space Agency (ESA) has addressed an envisioned need for advanced gain scheduling techniques in Space by establishing industrial-academia consortiums tasked with developing an industrial LPV control design framework supported with reliable LPV software tools. The LPV Modeling, Analysis and Design (LPVMAD) consortium lead by Deimos Space (Spain) and composed by research teams from the Computer and Automation Research Institute (SZATKI, Hungary), Delft Technical University (The Netherlands) and Leicester University (United Kingdom) was formed to address this need. The project objectives are:

i. To assess the possibility, needs and impact of LPV techniques in the control design process for space systems

ii. To propose a control design LPV framework

iii. To develop reliable LPV tools for modeling, analysis and design in support of such a framework

iv. To demonstrate the developed framework and tools for a relevant space system

Results from Phase I of the project [10, 11, 12, 13, 14, 15] detailed the successful accomplishment of the first three points above. Phase II of the project was tasked with addressing the 4th point above using a more challenging benchmark that included practical issues such as saturation, motion coupling, controller scheduling and time-varying behaviour. The selected benchmark was an enhanced version of the well-known NASA HL-20 atmospheric re-entry vehicle, which is detailed next.

A. LPVMAD re-entry benchmark: the enhanced NASA HL20

The HL-20 lifting-body vehicle was proposed as a substitute of the Space Shuttle Orbiter and although it was finally de-commissioned, many research efforts were performed to develop a fairly detailed baseline aerodynamic database for the complete speed range of the vehicle [2, 3, 4, 5]. In this section the development of the nonlinear implementation of the vehicle, including trajectory and models, is detailed.

A 3 Degrees-of-Freedom optimized guidance trajectory adapted from NASA reference [7] is considered. The LPVMAD project focused in the full aerodynamic phase corresponding to the terminal energy approach management (TAEM), approximately from low supersonic to a sub-sonic speeds for a range of Mach$\in$[3,0.8]. This selected phase represents the end of a bank reversal coupled with the roll-off from a 12 degrees angle of attack to a constant 4 degrees, see Figure II-1.

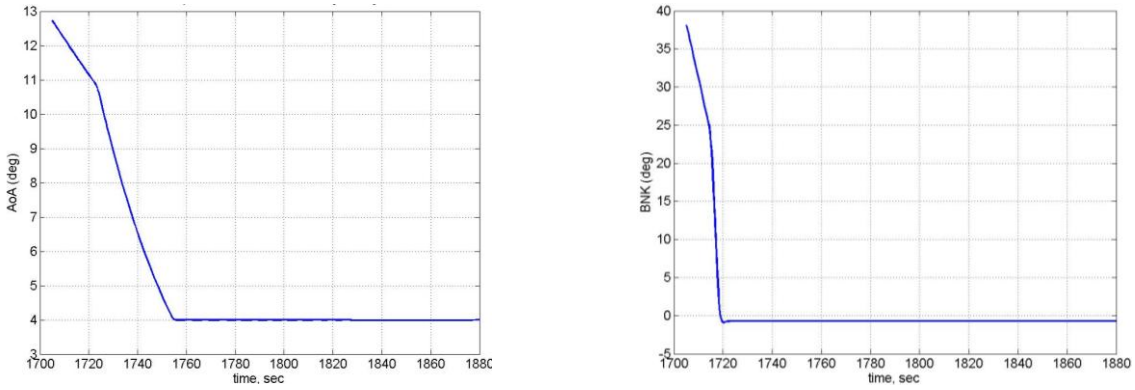

Figure II-1 Nominal reference trajectory: angle-of-attack and bank angle profiles versus time

The full nonlinear equations of motion, see reference [9] for details, are used together with a representative aerodynamic database (taken from NASA's reports [2, 3, 4, 5]). This HL-20 implementation is a quite more advanced, and representative, model than the publicly available Matlab model [6], which uses the polynomial simplifications given in NASA's report [3]. The complete aerodynamic database is formed by nonlinear look-up tables (LUT) dependent on Mach number, angle of attack, sideslip and control surface deflections [10].

The available control surfaces are upper left and right flaps (DUL and DUR), lower left and right flaps (DLL and DLR), wing left and right flaps (DEL and DER) and rudder (DR). The deflection is positive downward for the upper/lower flaps (+TED and -TEU), away from the vehicle for the wing flaps (+TED) and to the left for the rudder (+TEL). A control surface mix logic is implemented formed by nonlinear functions dependent on elevator deflection

δele, ailerons deflections *δail*, speed-brake deflection *δsbk*, rudder deflection *δrud* and Mach number, see [10]. The output from the control-mixer is passed to the actuation system, consisting for each actuation channel in a series connection of 2nd order dynamics, magnitude limiter, rate limiter and time delay (of 0.005 seconds). The sensor system is implemented as a first order coloured filter with measurement-dependent corner frequencies K and bias and being driven by Gaussian white noise (obtained using Matlab band-limited white noise generator with noise power of one and a sample time of 0.01 seconds).

A multiplicative uncertainty model is used, $u_{\Delta}=(1+\delta_U \Delta_{\%})u$, based on established percentage uncertainty range $\Delta_{\%}$, nominal values u and a normalized random gain δ_U. For those magnitudes with nominal value equal to zero, an additive model is employed (the multiplicative model would not introduce uncertainty in the parameter for these cases). Reference [10] details the nominal values and percentage uncertainty range used in the HL-20 re-entry vehicle benchmark for the main vehicle geometry and aerodynamic parameters: center of gravity coordinates, moments of inertia, mass and aerodynamic coefficients –including a $C_{L/D}$ uncertainty profile that serves to physically relate the uncertainties from CL and CD. Further, the aerodynamic database (as given in NASA reports [2, 3, 4, 5]) is quite nonlinear and alternates stable with unstable phases – notice the positive and negative slopes in C_{MO} from Figure II-2.

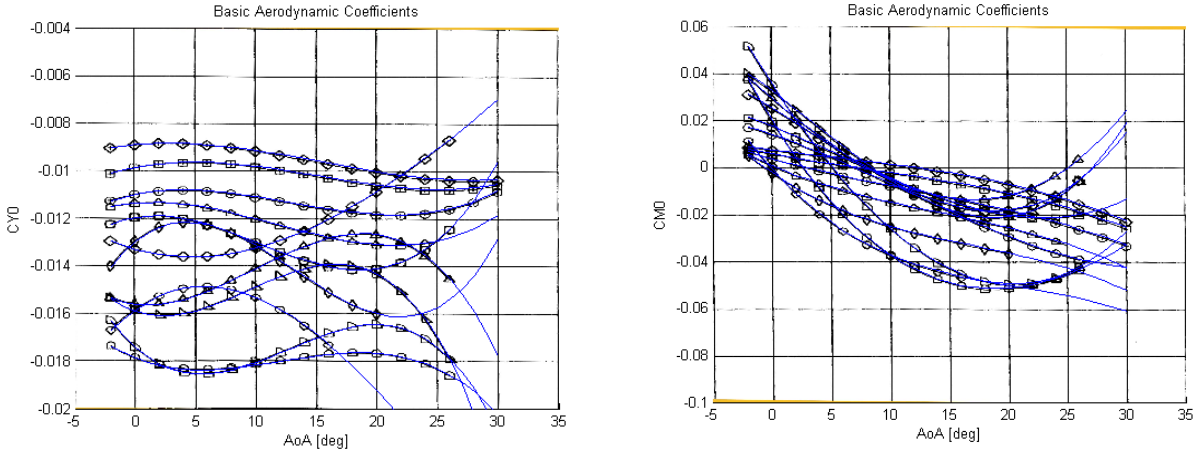

Figure II-2 Enhanced HL-20: basic aerodynamic coefficient in terms of angle-of-attack and Mach

A detailed analysis of the dynamic characteristics of the benchmark is given in [10], which shows that the vehicle is quite challenging with shifts in stability for the lateral/directional and longitudinal motions with strong natural frequency and DC gain changes as the vehicles flies down the trajectory, see for example Figure II-3.

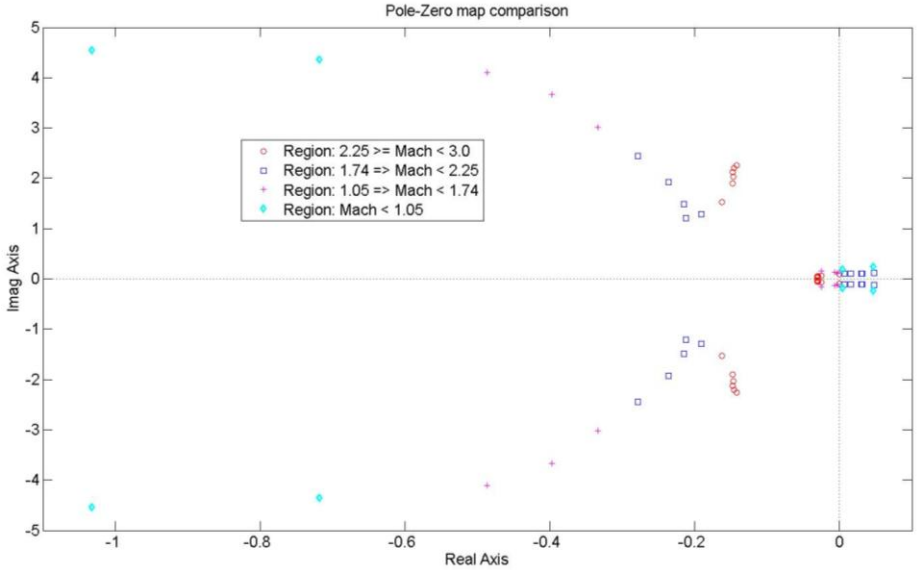

Figure II-3 Enhanced HL-20 lat/dir motion dynamic change: Pole/Zero map based on Mach regions

III. Baseline Control Law Design: Gain-Scheduled LTI H_∞

This chapter presents the gain-scheduled LTI H_∞ baseline control design. The approach tries to follow as much as possible the most standard assumptions and methodology, thus it is assumed a decoupled motion and incremental design complexity. Due to the characteristics of the system it is not possible to design a single LTI H_∞controller for each motion that provides acceptable global performance for the full motion. Thus, ad hoc gain scheduling of several, across Mach, LTI H_∞ point designs is performed.

LTI H_∞ is a design technique where specification of performance and robustness objectives is the main driver in correctly posing the mathematical optimization problem (as opposed to other control synthesis techniques where satisfaction of the objectives is evaluated after the design). LTI H_∞ control synthesis is indeed one of the cornerstones of modern control and is widely used across industry. The LTI H_∞ point-design synthesis problem follows two specific steps:

- Posing of the H_∞ interconnection framework. The H_∞ interconnection represents the main mathematical framework for subsequent optimization. It specifies the input and output channels and establishes the design rationale, e.g. ideal model matching. The idea behind the H_∞ interconnection is for the designer to establish the transfer functions that the optimizer will try to minimize in synthesizing the controller to achieve the desired closed-loop behaviour (e.g. sensitivity and complementary sensitivity responses).
- Weight design. The H_∞ interconnection contains the so-called weights, which are used to map the performance and robustness design specifications into the mathematical framework. The weights are (typically) first or second order transfer functions that the designer uses to shape the problem. The general ideas behind weight design are:
    - Noise weights. Typically high-pass weights to indicate the high-frequency noise associated with measurement units. These weights can be used to fine-tune the robustness of the closed loop.
    - Actuator weights. They are used to bound the controller output channel effort and for robustness purposes (i.e. they are used to shape the complementary sensitivity). As a first approximation, the inverse of the maximum deflections and rates for the actuators are typically used.
    - Error/performance weights. These weights, together with ideal models, represent the main performance tuning knobs. They are mainly low-pass functions whose inverses bound the sensitivity function.
    - Ideal/command-shaping weights. First and second order low-pass weights (usually based on flying/handling qualities specifications) that contribute to shape the bandwidth and performance of the closed-loop.

The incremental design step to achieve a global controller that follows from the single design-point H_∞synthesis is to combine a set of LTI designs. The most widespread approach is that of gain scheduling, which augments the above steps with an additional one. The main steps of gain-scheduled LTI H_∞ synthesis problem are:

- Obtain LTI point-design controllers across the flight envelope using a set of scheduling parameters that measure the change in dynamics. These point-designs can be obtained by any control design technique but in the present case, we use the LTI H_∞ synthesis process as described above. The key issues in this step, besides the actual synthesis, are: the selection of the points across the flight envelope at which to perform the designs, and setting the gain-scheduled framework (e.g. state-space matrices or controllers' output interpolation). The latter issue is more appropriately considered within the next step but we introduce it here as its definition has a critical influence on the individual design-point synthesis. For example, output interpolation will require that the controllers share a common set of outputs while state-space matrix interpolation requires that they share the same input/output/state structure.
- Gain-scheduling or interpolation of the point-design controllers. In the classical gain-scheduling process this step is ad-hoc and absorbs most of the designer's time without providing a guarantee on the performance and robustness of the global design. Key issues on this step are: selection of the scheduling parameters and selection of the interpolation rule.

The control design objectives are mainly to track the reference angles of attack, sideslip and bank in the face of the established noise and uncertain levels with desired deviations of less than 2 degrees, with acceptable short-term deviations of less than 4 degrees.

A. Longitudinal design

The design rationale for the industrial benchmark longitudinal motion is that of angle-of-attack tracking through an ideal-model formulation. Since only the inner-loop is considered, i.e. no guidance, the open-loop plant can be reduced to the short-period motion. In this manner, the state dimension of the controller is largely reduced (recall that for LTI H_∞, the obtained controller has the same number of states as found in the interconnection).

The open-loop plant used for design has 2 states (angle-of-attack and pitch rate), two outputs (same as the states) and two inputs (elevator and speed-brake deflections). The defined H_∞ interconnection is given in Figure III-1. *Wact* penalizes the actuators magnitude; *Wrob* is used to add uncertainty at the plant input; *Wperf* and *Wid* serve to capture the angle-of-attack tracking formulation and to penalize its error; *Wcmd* shapes the angle-of-attack input; And finally, *Wnoise* is used for robustness by shaping the noise effect on the system. The *I*-block is introduced to indicate that no model of the actuators was used in the synthesis. The values of the final weights used in the synthesis are given later in Table III-1**.**

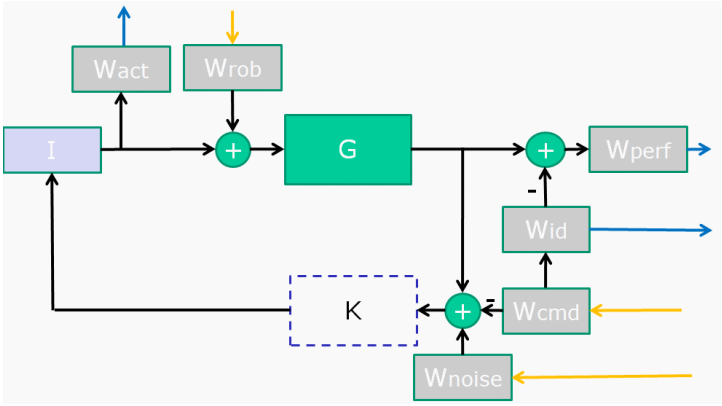

Figure III-1 Enhanced HL20 longitudinal baseline controller: H-infinity design interconnection

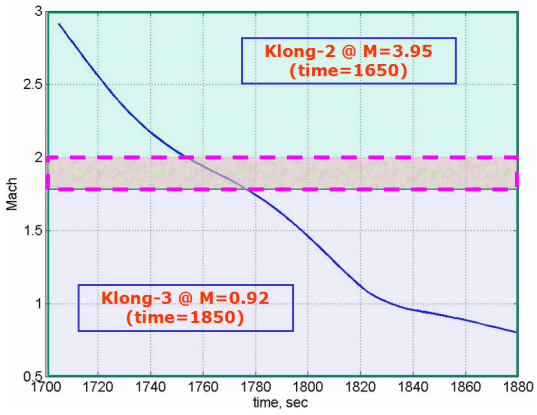

Figure III-2 Enhanced HL20 longitudinal baseline controller: scheduling

For the decoupled longitudinal motion (leaving the lateral/directional loop open), it is possible to design an acceptable single LTI H_∞ from Mach 20 down to Mach 0.8. But when closed with any lateral/directional controller, the interaction issues between the longitudinal and lat/directional aerodynamic surfaces (arising from the control-mixer) yields unacceptable loss of performance (which invalidates the standard decoupled motion assumption). Rather than using a coupled design approach, and in order to keep as close as possible to the standard design process, a gain-scheduled approach is preferred.

The scheduling parameter used is Mach number, which captures well the dynamic changes of the system and is relatively a standard measurable signal. The LTI design-points are selected by starting at the upper extreme in the trajectory, synthesizing a controller at that point, and then analyzing its linear performance and robustness from a frequency and time domain perspective at other design-points along the trajectory until performance is lost. Once this occurs, weight redesign is attempted to enlarge the controller coverage repeating the synthesis and linear analysis steps until we are satisfied. It is relatively straightforward to establish the coverage of a LTI H_∞ controller by proceeding in this manner, although of course more time can be dedicated to fine-tune the controller in order to enlarge its coverage or to improve its performance/robustness characteristics. Based on the analysis performed for a given design point, the next point is selected so that it overlaps the tail end of the previous controller valid region and the same process is repeated until the full trajectory is covered. Additional analysis tools, such as the nu-gap are used at the beginning of the design process to provide a quantified indication of the potential design regions. Figure III-2 shows a graphical representation of the design-point controllers' coverage and the associated interpolation region (we only show those from Mach 3.0 down to 0.8). The selected LTI H_∞ controllers (i.e. Mach numbers and corresponding nominal-trajectory times) are also indicated.

A controller output interpolation scheme is selected. This has the advantage of avoiding numerical issues with the state-space matrix interpolation as well as issues such as state convergence, dwelling time, initial condition and CPU load processing. The key issue in controller output interpolation is to ensure that wind-up does not occur, and this is accomplished by ensuring the deflection magnitudes are relatively of similar size and sign (i.e. avoiding one controller demanding +20deg deflection and the other -20deg for the same surface). The rule followed is linear interpolation based on Mach number. The selection of the specific Mach numbers at which to perform the interpolation is a non-trivial issue. It involves repeated design iterations and examination not only of linear analysis responses but also, and mostly, of the gain-scheduled controller behaviour in the nonlinear closed-loop for a set of worst-cases and a set of random simulations. Initially, only min/nom/max uncertainty cases are used for the worst-case set together a set of 50 random uncertainty cases. As failed uncertainty cases are discovered during the repeated design/validation cycle, they are added to the worst-case set and a new set of 50 random cases is generated. A different approach is to use physically oriented worst-case sets, i.e. worst-on-worst combinations of mass/inertia/cg parameters, but the approach followed serves to obtain additional information on the controllers' shortcomings as they are being designed.

With respect to the weight design, the interconnection from Figure III-1 is used together the weights design guidelines previously given. We start with the weight design for the first design-point ($Klong_1$ at Mach=22.71) and once a set of weights is satisfactorily defined, we follow the gain-scheduled process modifying these initial weights for each new design-point. The design includes an ideal second order model with a desired damping of 0.9 and natural frequency of 1.5 radians/second. Table III-1 shows the weights for the three longitudinal design-point controllers in terms of the generic weight transfer function of Eq (9). For $Klong_2$ and $Klong_3$ only the modified weights (with respect to those from $Klong_1$) are given.

$$W = K\frac{as+1}{bs+1} \tag{1}$$

Table III-1 Enhanced HL20 longitudinal baseline controller: H-infinity weight

Type	Weight	$Klong_1$			$Klong_2$			$Klong_3$		
		K	a	b	K	a	b	K	a	b
Noise	$W_{\alpha\text{-noise}}$	0.01*d2r	0	0						
	$W_{q\text{-noise}}$	0.001*d2r	1000	100				0.01*d2r	100	10
Ideal/cmd	W_{ideal}	1.5^2 / (s^2 + 2*0.9*1.5*s +1.5^2)								
	W_{cmd}	2*d2r	0.6667	2				2*d2r	0	0
Performance	W_{perf}	150	1	10	150	0	10	150	0	0
Robustness	$W_{rob\text{-}ele}$	0.01	0	10						
	$W_{rob\text{-}sbk}$	0.01	0	0						
Actuation	$W_{act\text{-}ele}$	1/60/d2r	0	0				1/40/d2r		
	$W_{act\text{-}sbk}$	1/20/d2r	0	0				1/60/d2r		

B. Lateral/Directional design

The lateral/directional open-loop plants used for the design has four states (yaw rate r, roll rate p, sideslip angle β and bank angle ϕ), two input channels (aileron δ_{ail} and rudder δ_{rud} deflections) and four outputs (yaw rate, roll rate, lateral acceleration n_y and bank angle).

The interconnection used is shown in Figure III-3. It is based on a model-matching approach for bank angle commands (W_{cmd} and W_{id}) and includes two additional objectives within the performance weight W_{perf}: lateral acceleration minimization and turn-coordination. The latter performance objective is represented as $TC=r-0.037\phi$ following [1, 8]). In what turned out to be a key difference with respect to the longitudinal design, a first-order model of the actuators *act* is used in addition to actuator weights W_{act} –which besides the magnitude, and more

importantly, also included limits on the actuators rate. The robustness weight W_{rob} is used to add uncertainty to the input of the plant in order to handle the challenging parametric and aerodynamic uncertainties.

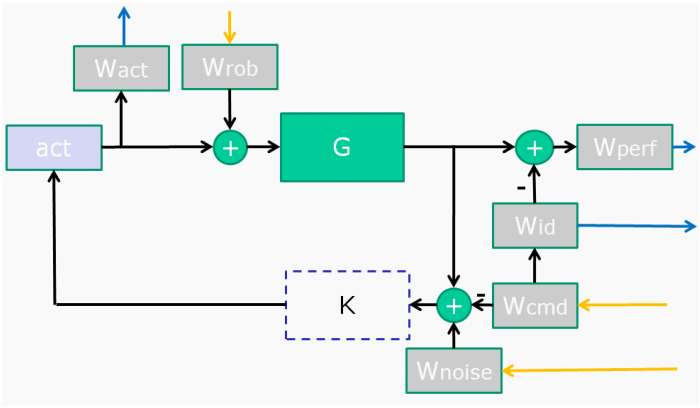

Figure III-3 Enhanced HL20 Lat/Dir baseline controller: design interconnection

As mentioned above, all attempts to design a single LTI controller for this motion are nil and furthermore, due to the control mix logic which directly couples the aileron and elevon demands the design of the de-coupled lateral/directional and longitudinal controllers is quite iterative and ad hoc. Following the approach for the longitudinal motion, the gain scheduling design process starts by selecting the highest Mach in the focused trajectory and establishing its coverage region before proceeding to the next point-design. Due to the richer dynamic and uncertain variations of this motion a larger number of interpolating LTI design points is necessary, i.e. any single LTI H_∞ lateral/directional controller had a smaller coverage region than those for the longitudinal motion. Table III-4 shows the weights for the four interpolating designs whose descriptions follow also the generic weight transfer function given in Eq (9), while Figure III-5 shows the interpolating regions.

Table III-4 Enhanced HL20 lat/dir baseline controller: H-infinity weight

Type	Weight	$Klat_1$			$Klat_2$			$Klat_3$			$Klat_4$		
		K	a	b	K	a	b	K	a	b	K	a	b
Noise	$W_{p=}\ W_r$	0.01*d2r	0	0									
	W_σ	0.01*d2r	0	0									
	W_{ny}	0.01/9.8	0	0				0.5/9.8					
Ideal/cmd	W_{ideal}	1.03	0	0.5886				1.075	0	0.6143	1.04	0	0.5943
	W_{cmd}	15*d2r	1	10				25*d2r	1	1.6667	25*d2r	1	1.6667
Performance	W_{ny}	0.1	0	0				2.9	0	0			
	W_ϕ	103	0.5	10.3				107.5	0.5	21.5	103	0.5	20.6
	W_{TC}	2	0	0									
Robustness	W_{ail}	1*d2r	0	0.1	0.2*d2r	0	1						
	W_{rud}	1*d2r	0	0.1	0.2*d2r	0	1	0.02*d2r	0	0.2			
Actuation	W_{ail}	0.005/d2r	0	0.1	0.015/d2r	0	1	10*d2r	0	0	1*d2r	0	10
	W_{rud}	0.005/d2r	0	0.1	0.015/d2r	0	1	1*d2r	0	0	1*d2r	0	10
	$W_{ail\text{-}dot}$	0.005/d2r	0	0	0.01/d2r	0	0	0.35*d2r	0	0	0.5*d2r	1	10
	$W_{rud\text{-}dot}$	0.005/d2r	0	0	0.01/d2r	0	0	0.35*d2r	0	0	0.5*d2r	1	10

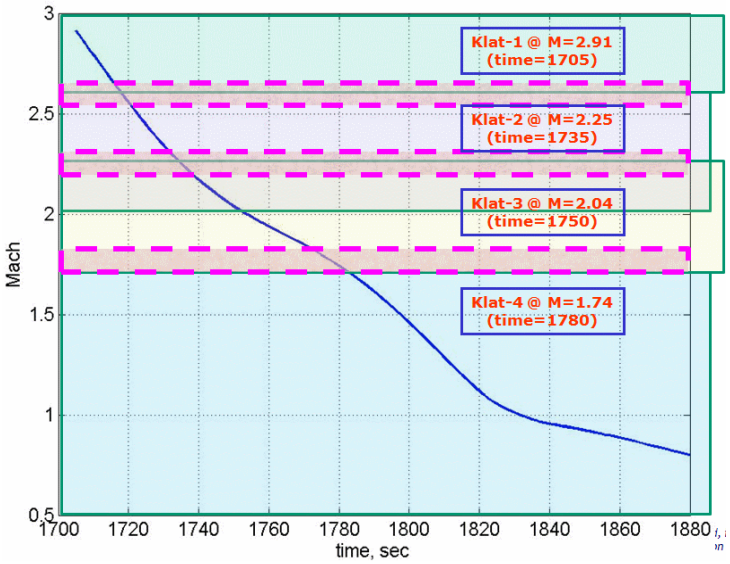

Figure III-5 Enhanced HL20 lat/dir baseline controller: scheduling

IV. Design Cycle Linear Analyses

At each design step, the linear analyses presented in this section are performed to assess the validity and coverage region of the obtained LTI H_∞ controllers. Some of the analyses serve to assess the proper control design requirements definition and satisfaction, such as those from Figure IV-1 and Figure IV-2, while others examine the controller characteristics such as the GK transfer function of Figure IV-3, and yet others look at its performance and robustness characteristics, Figure IV-4 and Figure IV-5. A mix of longitudinal and lateral/directional analyses is presented for illustration purposes.

Figure IV-1 shows the weighted performance of the transfer functions from the command [α_{cmd}] and noise inputs [q_{noise}, α_{noise}] to the performance error [α_{error}] for the longitudinal baseline design-point LTI controllers. The inverse of the performance weight is included to graphically ensure that the desired performance is satisfied. The left plot shows the analysis performed for *Klong*$_2$ (designed at *M=3.95*) using LTI plants at *M=[3.9591, 2.9127, 2.2503, 2.0384, 1.8465]*, and the right plot those for *Klong*$_3$ (designed at *M=0.92*) with LTI plants at *M=[1.8465, 1.4573, 1.0525, 0.9229, 0.82114]*. The validation LTI plants used for each controller determine their coverage region. Figure IV-2 shows the equivalent analysis for the actuation requirements, but for the lat/dir LTI point controllers.

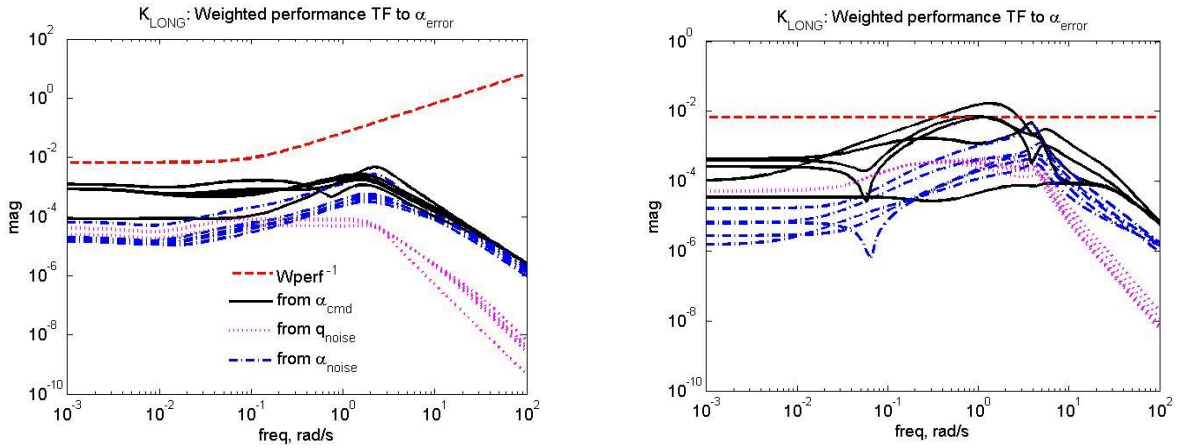

Figure IV-1 Enhanced HL20 longitudinal baseline controller: weighted performance TF to α_{error} Klong2 (left) – Klong3 (right)

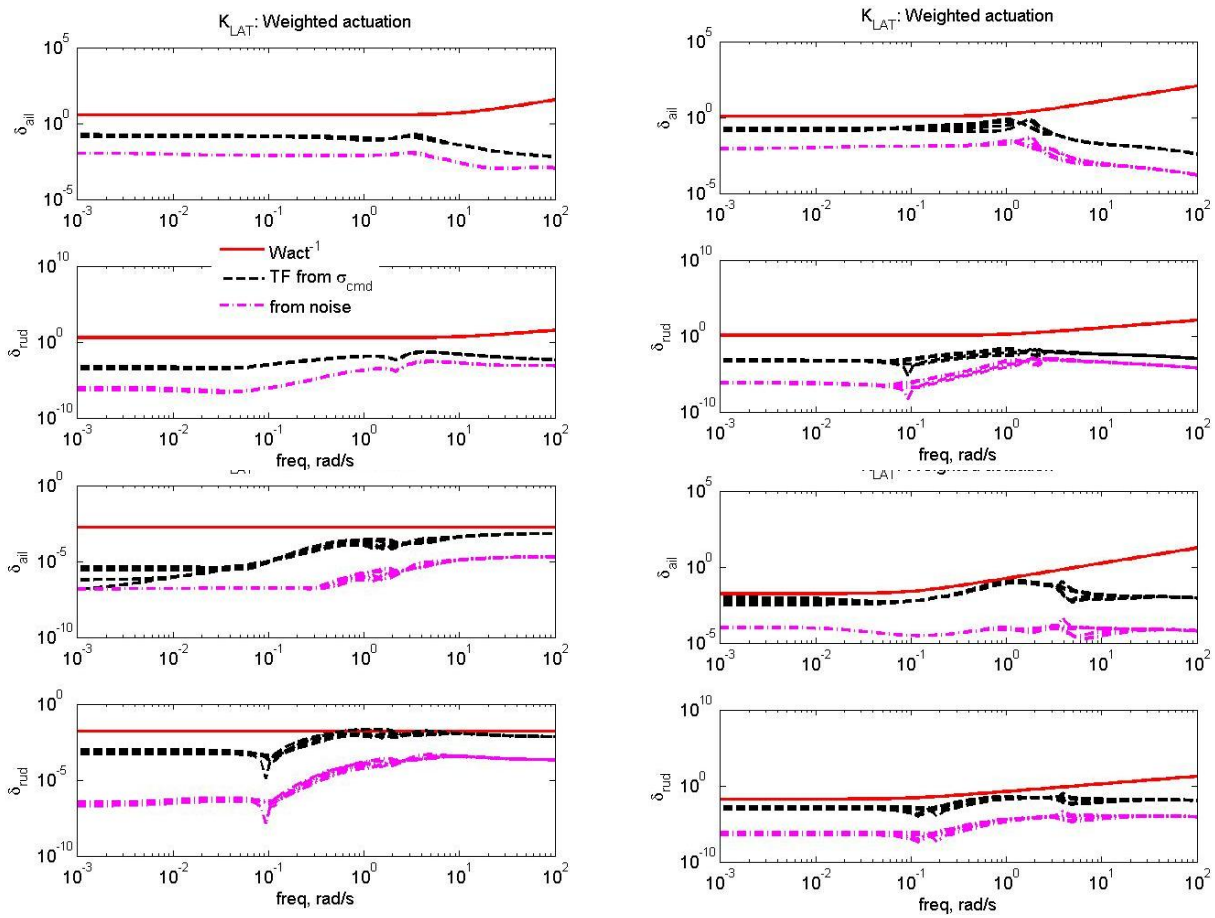

Figure IV-2 Enhanced HL20 lat/dir baseline controller: weighted actuation
Klat1 (top-left) – Klat2 (top-right) – Klat3 (bottom-left) – Klat4 (bottom-right)

Figure IV-3 shows the GK loop of the longitudinal LTI controllers. The figure indicates that good DC gain and roll-off is achieved for all the LTI plants tested, with all having a desired similar profile and value. Note that for *Klong*$_2$ (left plot) one plant starts to roll off at a lower frequency values, this type of information is used during the design process to identify and improve the controller coverage.

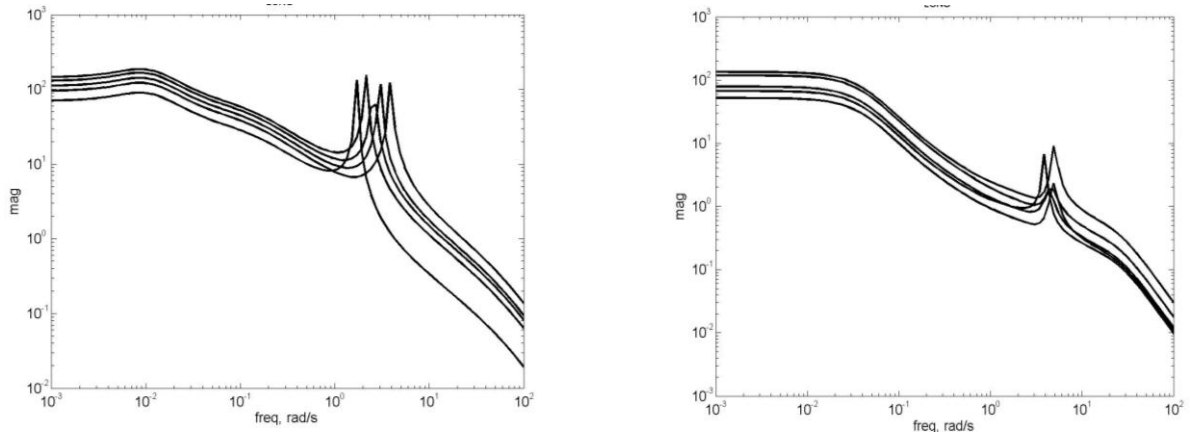

Figure IV-3 Enhanced HL20 longitudinal baseline controller: GK
Klong2 (left) – Klong3 (right)

With respect to the performance/ robustness of the controller, Figure IV-4 shows the lateral/directional controllers complementary sensitivity and sensitivity (T&S) responses in the left column –including performance/robustness weights for visualization of the design objectives' satisfaction – and the flying qualities (bounded linear step response) in the right. Note that the flying quality plots provide the coverage region information in terms of Mach numbers of the LTI plants used to obtain the step responses.

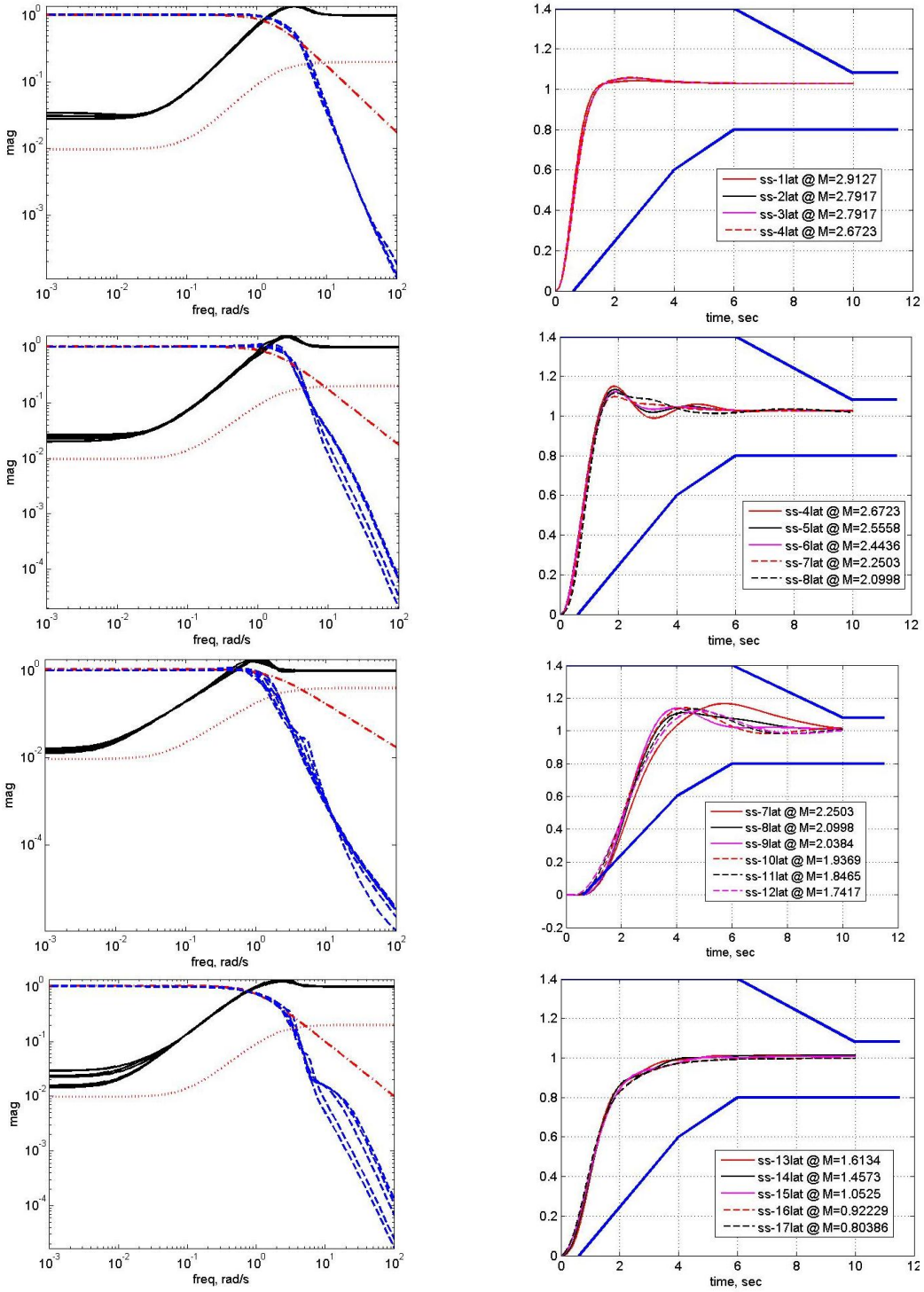

Figure IV-4 Enhanced HL20 lat/dir baseline controller: S&T and Flying Qualities
From top-to-bottom rows: Klat1 → Klat2 → Klat3 → Klat4

Finally, Figure IV-5 examines the linear simulation responses of the designed controllers, in this case for the longitudinal case. The simulation is performed in Simulink using the corresponding LTI H_∞ controller with a selected LTI plant but using the full actuator and sensor models described in the previous sections (including magnitude and rate saturation limits). An angle of attack command formed by a doublet followed by a ramp allows determining the 0 and 1-type response of the controllers. It is highlighted that both types of command are critical to satisfy the tracking error objectives of less than 2 degrees.

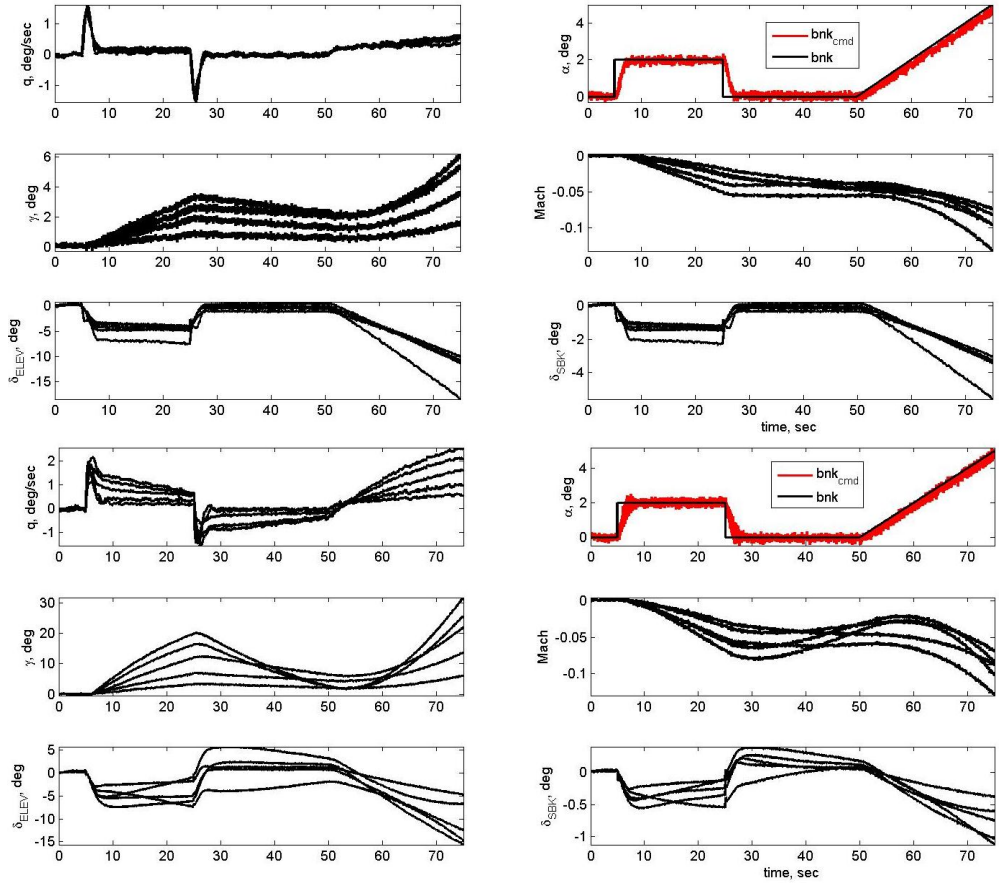

Figure IV-5 Enhanced HL20 longitudinal controller: linear responses (with full actuators & sensors) Klong2 (left) – Klong3 (right)

V. Nonlinear Time Simulations

In this section the full-motion gain-scheduled baseline control design is tested using the full nonlinear simulator of the re-entry HL20 vehicle. The first three plots show the outputs and tracking errors for the min/nom/max uncertainty cases while the last four show the results from a Monte Carlo campaign with a 1000 runs (although for figure size limitations only a 100 of the cases are shown in the plots, the remaining ones are of similar value).

A. Nominal, minimum and maximum uncertainty cases

Figure V-1 and Figure V-2 show respectively the longitudinal and lateral/directional outputs, while Figure V-3 shows the resulting inner-loop angle tracking errors (i.e. angle of attack, sideslip and bank angle). For the longitudinal case observe the two clearly visible regions in the pitch rate and angle of attack plots where oscillations occur, around time 1720 and around time 1760 seconds. For the lateral/directional case, we observe a strong oscillatory region from 1740 to 1750 seconds. These regions are the result of coupling between the motions and of controller interpolation, both issued only accounted for indirectly through ad hoc controller retuning and interpolation. Indeed, it is noted that most of the time devoted to the baseline controller design was spent trying to compensate in an ad hoc manner for the coupling issue and on the selection of the proper interpolation values.

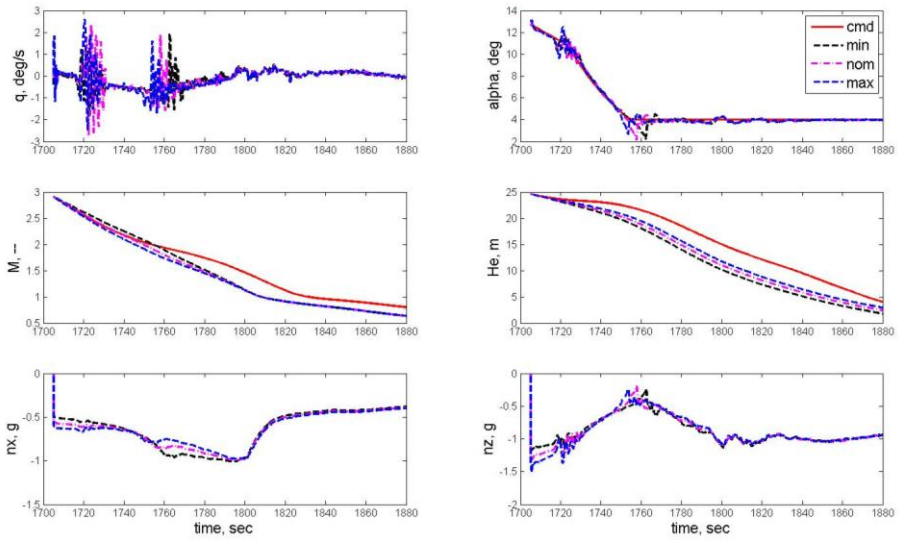

Figure V-1 Nonlinear min/nom/max-Δ full baseline controller: longitudinal outputs

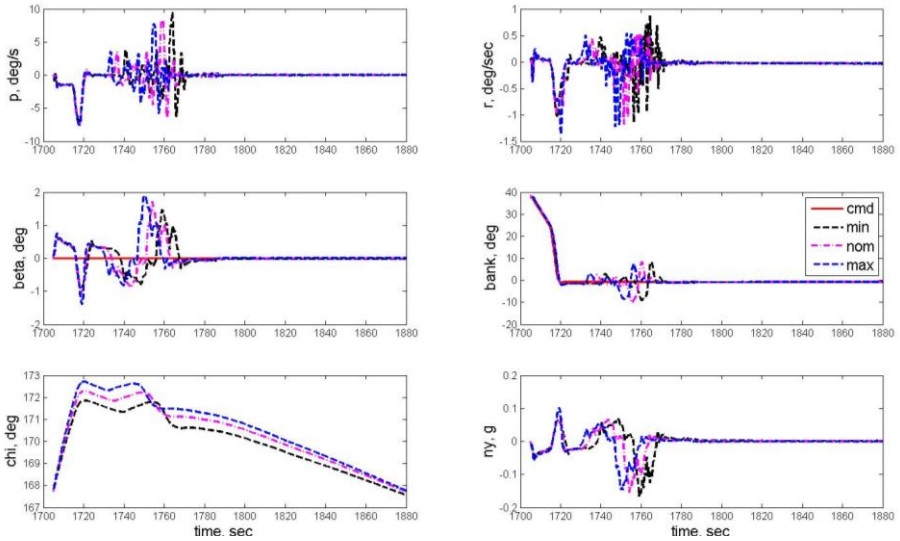

Figure V-2 Nonlinear min/nom/max-Δ full baseline controller: lateral/directional outputs

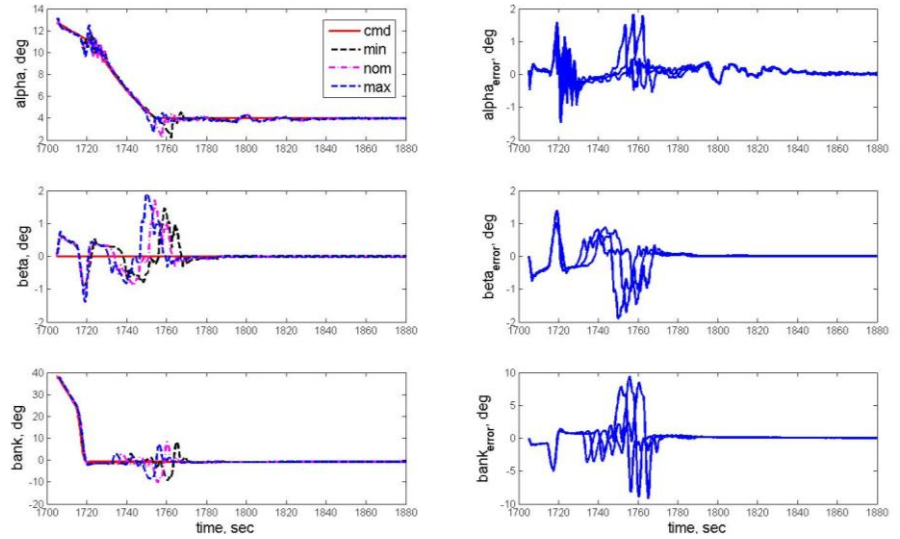

Figure V-3 Nonlinear min/nom/max-Δ full baseline controller: tracking signal errors

B. Monte Carlo campaign

The baseline controller validation concludes with a Monte Carlo (MC) campaign of the controller using the full motion nonlinear simulator. The MC uses 1000 random runs covering the full 100 percent uncertainty ranges [10], with 7% cases failing (not shown in the plots). An additional 400 random cases are tested, half of them using a 90% coverage of the uncertainty range and the other half at 80%. The corresponding numbers of failed cases are 5% and 2% indicating that the baseline controller is robust but that it does not fully satisfy the full robustness objectives. It is worth mentioning that the min/nom/max uncertainty cases from the previous three plots do not reveal this shortcoming on the controller robustness. Figure V-7 shows the MC tracking angle errors that clearly show in the case of the bank angle error, that neither the desired ±2 degrees error nor even the acceptable ±4degrees error objectives are satisfied. Nevertheless, for the purposes of the controller design –that of serving as a baseline for advanced gain-scheduling control studies—the controller represents best-industrial practices and faces all the challenges associated to this type of vehicles.

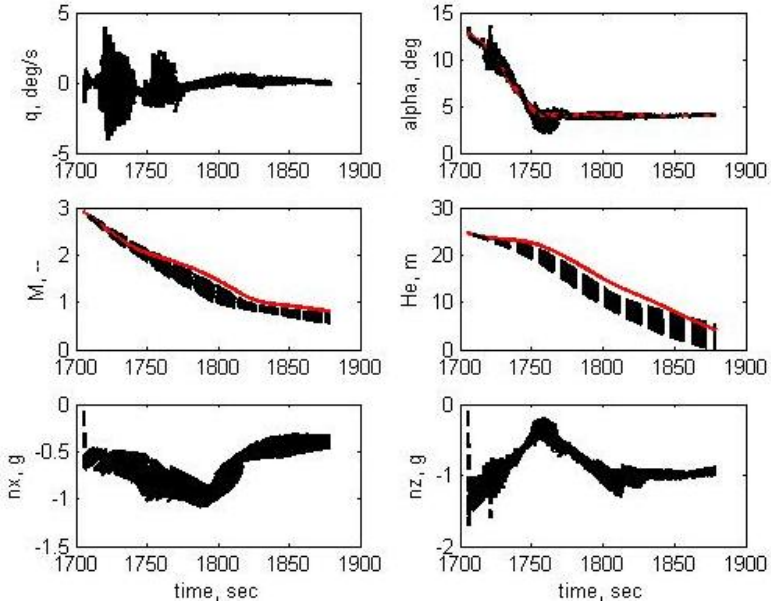

Figure V-4 Monte Carlo full baseline controller (100 out of 1000 runs): longitudinal outputs

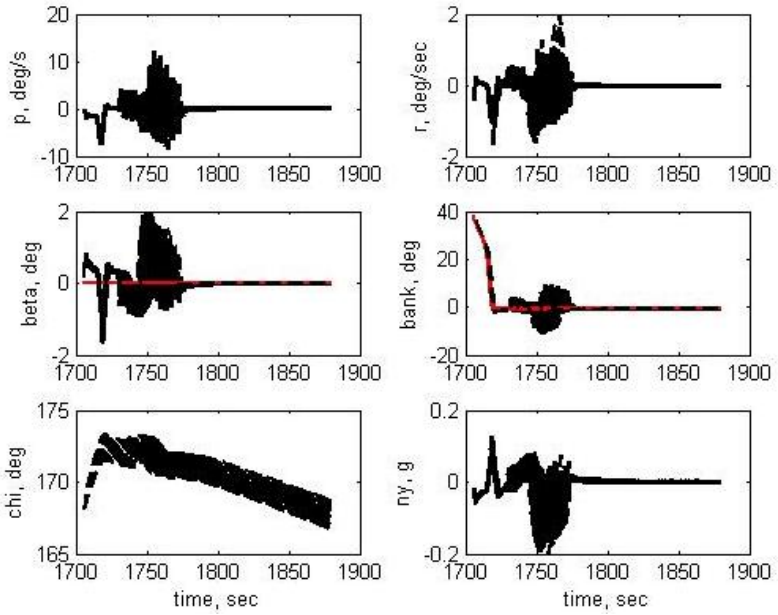

Figure V-5 Monte Carlo full baseline controller (100 out of 1000 runs): lat/dir outputs

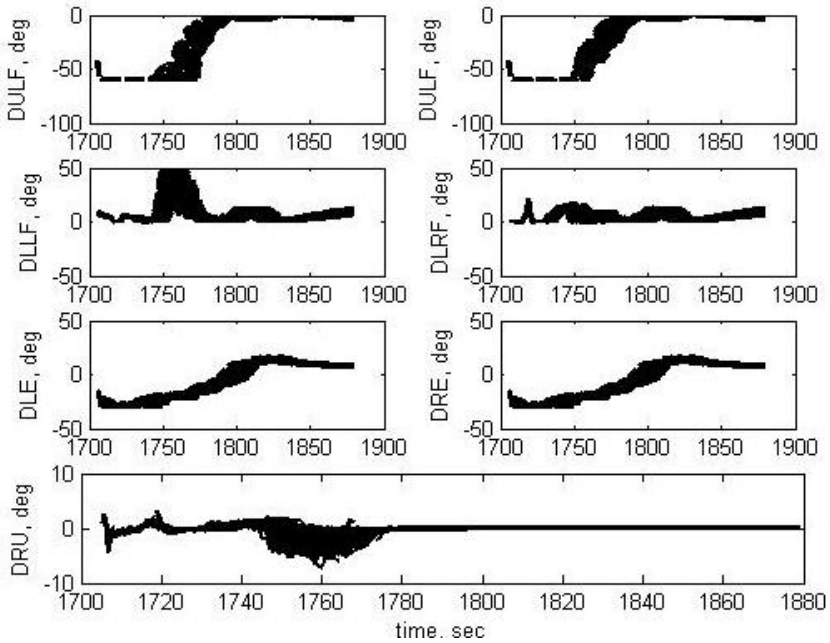

Figure V-6 Monte Carlo full baseline controller (100 out of 1000 runs): control surfaces

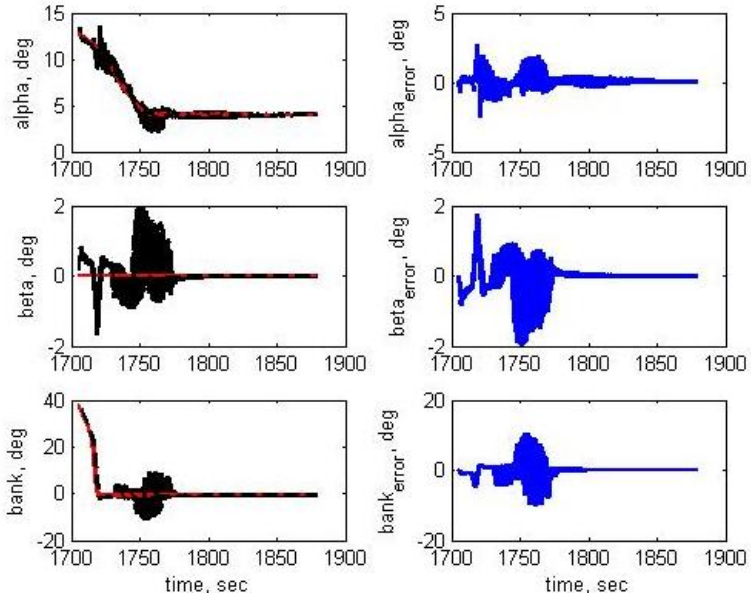

Figure V-7 Monte Carlo full baseline controller (100 out of 1000 runs): tracking signals

VI. Conclusion

In this article the design of a controller based on gain scheduling H_∞ has been presented for a re-entry benchmark. The controller was developed to serve as baseline controller design within the framework of a European Space Agency advanced gain-scheduling project. Detailed analyses and comments on the process and results are provided. The results showed that although full satisfaction of the control design objectives is not achieved, they are acceptable and more importantly illustrate the challenges faced in this type of vehicle. Improvement of the controller required only further weight and interpolation fine-tuning.

Acknowledgments

The author would like to thank the LPVMAD technical officer Dr. Samir Bennani from ESA-ESTEC for his help and comments. The LPVMAD project is funded by the European Space Agency under ESA-ESTEC contract 20565/07/NL/GLC.

References

1 Yamaguchi, Y., Ohara, A., Morito, T. "Flight Controller Design using IQC to Satisfy Stability Margin Requirements of MIMO System", AIAA GNC Conference 2001.

2 Jackson, E.B., Cruz, C.I., Ragsdale, W.A. "Real-Time Simulation Model of the HL-20 Lifting Body", NASA Langley Technical Memorandum 107580, July 1992

3 Jackson, E.B., Cruz, C.I. "Preliminary Subsonic Aerodynamic Model for Simulation Studies of the HL-20 Lifting Body" NASA Langley Technical Memorandum 4302, 1992

4 Cruz, C.I., Ware, G.M. "Control Effectiveness and Tip-Fin Dihedral Effects for the HL-20 Lifting-Body Configuration at Mach Numbers from 1.6 to 4.5", NASA Langley Technical Memorandum 4697, 1995

5 Scallion, W.I. "Aerodynamic Characteristics and Control Effectiveness of the HL-20 Lifting Body Configuration at Mach 10 in Air", NASA Langley Technical Memorandum 209357, September 1999

6 Gage, S. "HL20 aeroblockset MATLAB", The Mathworks

7 Powell, R.W. "Six-Degree-of-Freedom Guidance and Control-Entry Analysis of the HL-20" Journal of Spacecraft and Rockets, Vol.30, No.5, 1993

8 Doyle, J.C, Lenz, K., Packard, A.. "Design examples using mu-synthesis: Space shuttle lateral axis FCS during re-entry" IEEE Control Decision Conference, Vol 25, pp 2218-2223, December 1986

9 Marcos, A., De Zaiacamo, G., Mostaza, D., Kerr, M., Veenman, J., Scherer, C., Bennani, S., "Application to a re-entry vehicle of LPV/IQC modeling, design and analysis methods", AIAA GNC 2010.

10 Marcos, A., Kerr, M., De Zaiacomo, G., Peñín, L.F., Szabó, Z., Bokor, J., Rodony, G., "Application of LFT/LPV Modeling and Data-based Validation to a Re-entry Vehicle," AIAA Guidance, Navigation and Control Conference 2009

11 Marcos, A., Bennani, S., "LPV Modelling, Analysis and Design in Space Systems: Rationale, Objectives and Limitations," AIAA GNC Conference 2009

12 Menon, P.P., Prempain, E., Postlethwaite, I., Bates, D., Bennani, S., "An LPV loop shaping controller design for the NASA HL-20 re-entry vehicle," AIAA Guidance, Navigation and Control Conference 2009

13 Menon, P.P., Prempain, E., Postlethwaite, I., Bates, D., Bennani, S., "Nonlinear Worst-Case Analysis of an LPV Controller for Approach-Phase of a Re-entry Vehicle," AIAA Guidance, Navigation and Control Conference 2009

14 Veenman, J., Köroğlu, H., Scherer, C.W., "Analysis of the Controlled NASA HL20 Atmospheric Re-entry Vehicle based on Dynamic IQCs," AIAA Guidance, Navigation and Control Conference 2009

15 Veenman, J., Scherer, C.W., Köroğlu, H., "IQC-Based LPV Controller Synthesis for the NASA HL20 Atmospheric Re-entry Vehicle," AIAA Guidance, Navigation and Control Conference 2009

16 Rugh, W.J., Shamma, F., "Research on Gain Scheduling," Automatica, Vol. 36, 2000, pp. 1401–1425

17 Leith, D.J., Leithead, W.E., "Survey of Gain-Scheduling Analysis and Design," International Journal of Control, Vol. 73, No. 11, 2000, pp. 1001–1025

18 Balas, G.J., "Flight control law design: An industry perspective", European Control Conference, September 2003